



New Developments in Thermal Dispersion Mass Flow Meters

Presented at the American Gas Association Operations Conference
Pittsburgh, PA May 20-23, 2014

By John G. Olin, Ph.D., Founder/Chairman, Sierra Instruments

A S I E R R A W H I T E P A P E R

www.sierrainstruments.com

NORTH AMERICA

5 Harris Court, Building L / Monterey, CA 93940 / USA
800.866.0200 / 831.373.0200 / fx 831.373.4402

EUROPE

Bijlmansweid 2 / 1934 RE Egmond aan den hoef / The Netherlands
+31 72 5071400 / fx +31 72 5071401

ASIA - PACIFIC

Second Floor Building 5 / Senpu Industrial Park
25 Hangdu Road Hangtouw / Pu Dong New District
Shanghai, P.R. China Post Code 201316
+8621 5879 8521 / fx +8621 5879 8586

New Developments in Thermal Dispersion Mass Flow Meters

John G. Olin, Ph.D., Founder/Chairman, Sierra Instruments, Inc.⁽¹⁾

Presented at the American Gas Association Operations Conference, Pittsburgh, PA May 20-23, 2014.

Introduction

This paper describes a newly developed microprocessor-based thermal dispersion mass flow meter that uses four temperature sensing elements in its flow sensor instead of the traditional two elements and automatically manages changes in gas selection, gas temperature, gas pressure, and outside temperature. This new mass flow meter is ideally suited for apportionment applications in natural gas distribution systems.

Applications

Thermal dispersion mass flow meters measure the mass flow rate of fluids, primarily gases, flowing through a closed conduit. Their first general description is attributed to L. V. King who, in 1914 [1], published his famous King's Law revealing how a heated wire immersed in a fluid flow measures the mass velocity at a point in the flow. He called his instrument a "hot-wire anemometer." The first application of this technology was hot-wire and hot-film anemometers and other light-duty thermal dispersion flow sensors used in fluid mechanics research and as light-duty mass flow meters and point velocity instruments. This class of thermal dispersion mass flow meters is described in Reference 2.

It was not until the 1960s and 1970s that industrial-grade thermal dispersion mass flow meters emerged that could solve the wide range of general industry's more ruggedized needs for directly measuring the mass flow rate of natural gas, air, and other gases in pipes and ducts. That is the class of instruments described here. Thermal dispersion mass flow meters measure the heat convected into the boundary layer of the gas flowing over the surface of a heated velocity sensor immersed in the flow. Since it is the molecules of the gas, which bear its mass, that carry away the heat, thermal dispersion mass flow meters directly measure mass flow rate. Capillary tube thermal mass flow meters constitute a second type of thermal mass flow technology, but their principle of operation and their applications are sufficiently different that the American Society of Mechanical Engineers (ASME) has published separate national standards for each type [3] [4].

(1) SIERRA INSTRUMENTS, INC.
5 Harris Court, Building L / Monterey, CA 93940 / USA
800.866.0200 / 831.373.0200 / fx 831.373.4402
www.sierrainstruments.com

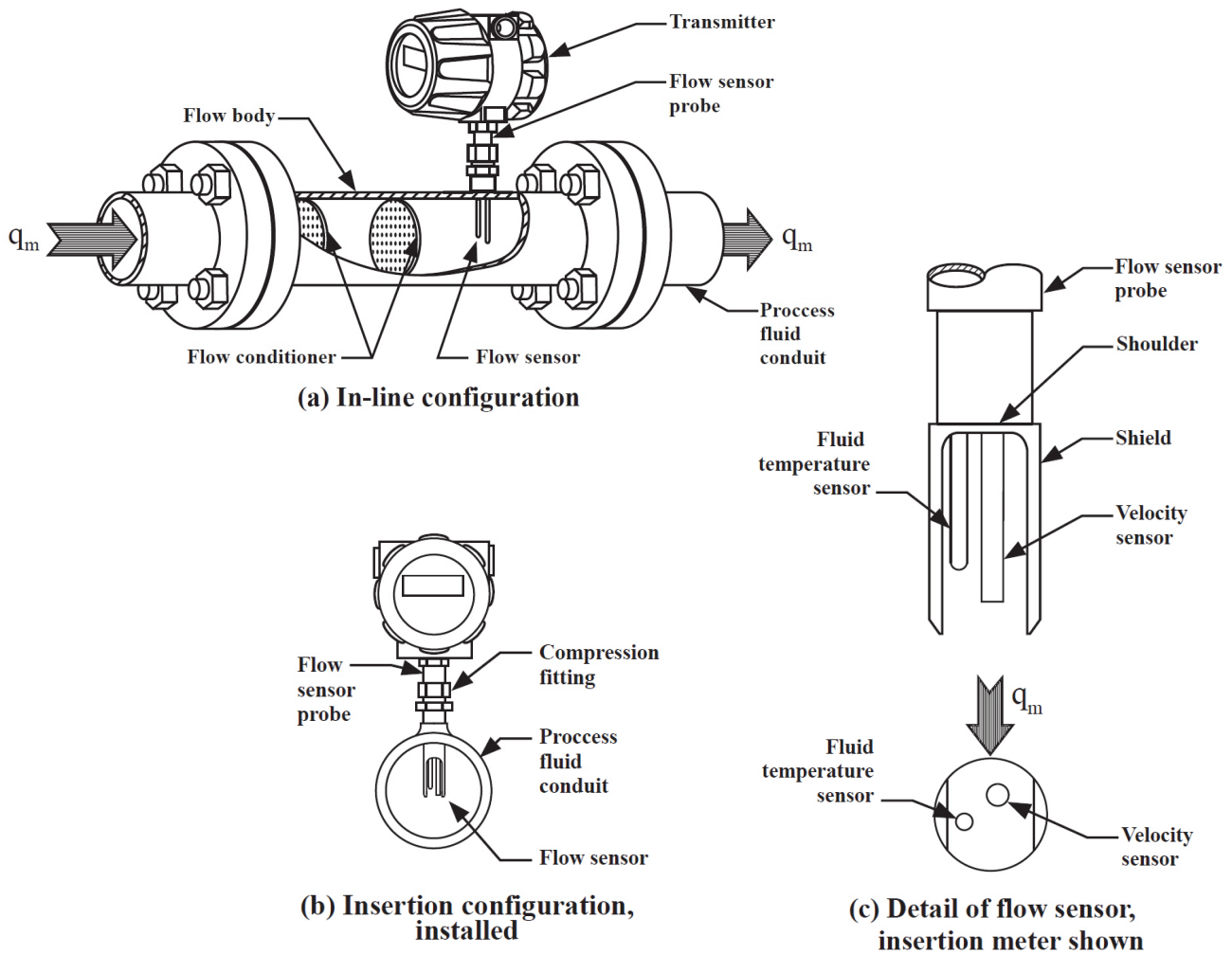


Figure 1 In-line and insertion meter configurations of thermal dispersion mass flow meters.

Typical gases monitored by industrial thermal dispersion mass flow meters include: natural gas, air, methane, carbon dioxide, nitrogen, oxygen, argon, helium, hydrogen, propane, natural gas, and stack gases, as well as mixtures of these gases and mixtures of hydrocarbon gases. Common applications are: natural gas distribution systems; combustion air; preheated air; compressed air; fluid power; boilers; electric power plants; cooling, heating, and mixing; drying of materials; food and beverage industries; aeration and digester gas monitoring in waste water treatment plants; cogeneration with biogas; fuel gas; flare gas; semiconductor manufacturing; heating, ventilation, and air conditioning; single and multipoint stack gas monitoring; and chemical reactors.

Table 1 Calculation of output variables for in-line flow meters

Variable	Units	Symbol	Formula
Mass flow rate, the primary output	kg/s	q_m	q_m from flow calibration
Mass flow rate, expressed as volumetric flow rate referenced to standard conditions () _s	standard m ³ /s	$q_{v,s}$	q_m/ρ_s
Volumetric flow rate	m ³ /s	q_v	q_m/ρ

General Description

Thermal dispersion mass flow meters directly measure the mass flow rate of single-phase pure gases and gas mixtures of known composition flowing through pipes or other flow conduits. As discussed in a later subsection, they also have limited application to single-phase liquids of known composition. In most of the following, we shall assume that the fluid is a gas, without the loss of applicability to liquids. Multivariable versions also provide an output for gas temperature and also, but less commonly, of gas pressure.

Thermal dispersion mass flow meters have two primary configurations: in-line and insertion. Figures 1(a) and 1(b), respectively, show these two configurations and their major components. Figure 1(c) shows the flow sensor that is common to both configurations, although in smaller in-line meters the flow sensor may not have a shield.

In-line flow meters are applied to pipes and ducts with diameters typically ranging from about 10 to 100 mm (0.25 to 4.0 inch pipe sizes), but some manufacturers offer sizes up to 300 mm (12.0 inch pipe size) . Process connections include flanges, pipe threads, and compression fittings. The built-in flow conditioner, described in Part 2 of this two-part series, reduces the length of upstream straight pipe required to achieve independence of upstream flow disturbances.

Insertion flow meters [5] usually are applied to larger pipes, ducts, and other flow conduits having equivalent diameters typically ranging from approximately 75 mm to 5 m. Because insertion meters are more economical than in-line meters, they also have found wide use as flow switches. Compression fittings and flanges are commonly used process connections. Insertion meters measure the mass velocity at a point in the conduit's cross-sectional area, but for applications with smaller conduits, they may be flow calibrated to measure the total mass flow rate through the conduit. Multipoint insertion meters measure the mass velocities at the centroids of equal areas in the cross section of large pipes, ducts, and

Table 2 Calculation of output variables for insertion flow meters

Variable	Units	Symbol	Formula
Point mass velocity, the primary output	standard m/s	V_s	V_s from Equation (15) or from flow calibration
Actual velocity	m/s	V	$(\rho_s/\rho)V_s$
Mass flow rate	kg/s	q_m	$\rho_s A_{\text{pipe}} F_c V_s$
Mass flow rate, expressed as volumetric flow rate referenced to standard conditions (ρ_s)	standard m ³ /s	$q_{v,s}$	$A_{\text{pipe}} F_c V_s$
Volumetric flow rate	m ³ /s	q_v	$(\rho_s/\rho) A_{\text{pipe}} F_c V_s$
Total mass flow rate for multipoint measurements in N equal areas	kg/s	q_m	$(\rho_s A_{\text{pipe}}/N) \sum_{i=1}^N V_{s,i}$

stacks. The total mass flow rate through the entire conduit is the average mass velocity of the several points multiplied by the total cross-sectional area and the standard mass density of the gas [6].

Advanced Flow Sensor

The flow sensor for the insertion flow meter shown in Figure 1(c) has a unique design incorporating an open-ended shield and a probe with a shoulder. Traditional insertion meters have a shield with a closed end that can cause the flow over the velocity sensor to be non-uniform and turbulent. The open-ended shield shown in Figure 1(c) protects the sensors but does not have this problem. Additionally, the probe in traditional insertion meters has a constant diameter and no shoulder. Whereas the largest portion of the flow around such traditional insertion probes flows circumferentially around the probe, a smaller fraction flows axially down the probe, enters the window in the shield, and passes over the velocity sensor, causing it to measure a velocity higher than the actual velocity in the flow conduit. Since the amount of this secondary flow varies with the depth of insertion into the flow stream, its magnitude during flow calibration may be different than that of the actual field application. This can impair the accuracy of velocity measurement. The probe in Figure 1(c) has a length of reduced diameter and a shoulder just above the flow sensor that redirects axial downwash so that it flows circumferentially around the probe before it can pass over the velocity sensor, thereby minimizing this source of inaccuracy.

Figure 2(a) shows a traditional thermal dispersion flow sensor used in in-line and insertion mass flow meters intended for industrial-grade applications. This flow sensor has a velocity sensor and a separate temperature sensor immersed in the flow stream. For that reason, thermal dispersion mass flow meters are also named “immersible” thermal mass flow meters. The velocity sensor has a single electrically self-heated temperature sensor element located in its tip that both heats the velocity sensor and measures its

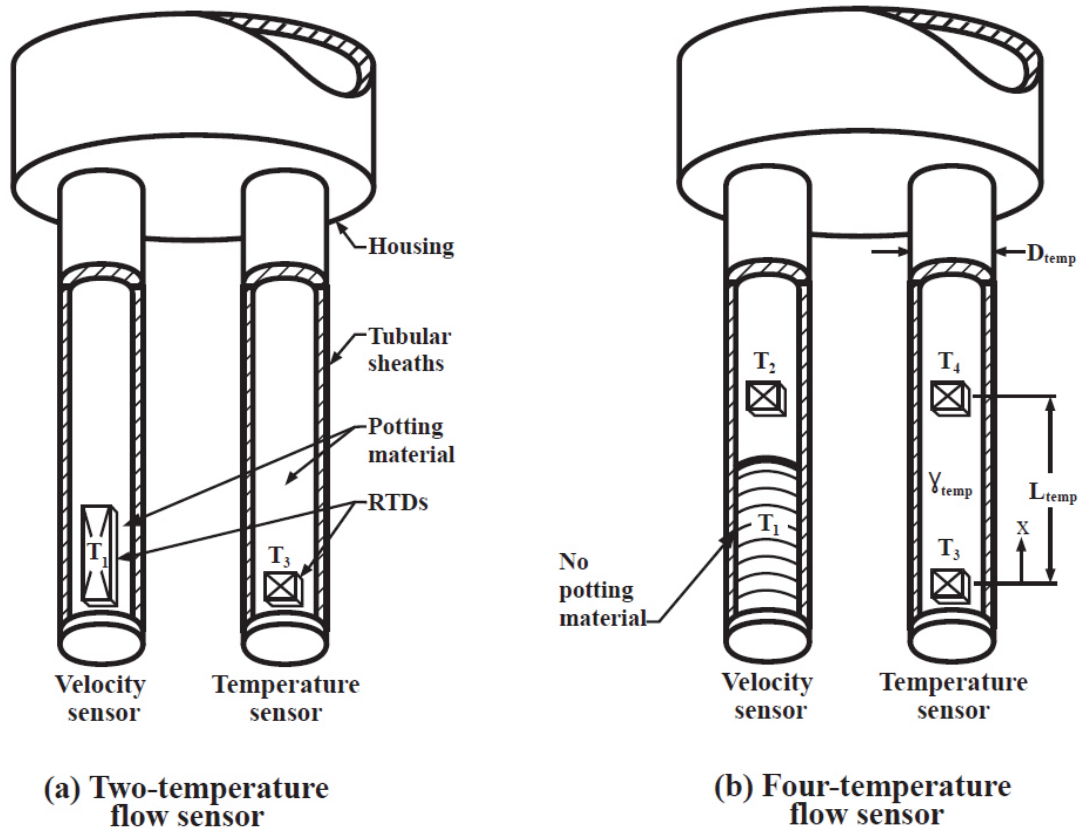


Figure 2 Two kinds of thermal dispersion mass flow sensors.

own average temperature T_1 . The gas temperature sensor has a single non-self-heated temperature sensor element T_3 located in its tip that measures the gas temperature T . Because it has a total of two temperature sensing elements, the flow sensor in Figure 2(a) is called a “two-temperature” flow sensor. The velocity sensor and the temperature sensor are mounted side-by-side. Each is enclosed in a rugged, sealed, single-ended, corrosion-resistant metallic tube, usually composed of 316 stainless steel or a nickel alloy. The introduction of this kind of rugged construction in the 1960’s and 1970’s is responsible for transforming thermal anemometers into industrial-grade instruments. In traditional velocity sensors of the kind shown in Figure 2(a), the T_1 sensor is potted into the tip of the tubular sheath. Typically, the potting, or filler, material is ceramic cement or epoxy. Heat sink grease also has been used for this purpose.

For higher accuracy and higher stability applications, the temperature sensing elements in the velocity sensor and the temperature sensor in Figures 2(a) and 2(b) are either wire-wound or thin-film platinum resistance temperature detectors (RTDs) protected by a thin insulation layer of glass or ceramic. The

electrical resistance of RTDs increases as temperature increases, providing the means for transducing their electrical output into temperature. The platinum RTD sensor element in the velocity sensor is called the T_1 element and has a relatively low electrical resistance in the range of about 10 to 30 Ohms. The platinum RTD element in the temperature sensor is called the T_3 element and has a relatively high electrical resistance in the range of 300 to 1000 Ohms. Other types of temperature sensing elements, such as thermistors, thermocouples, and micro-electronic machined devices, have been used for applications with lower accuracy requirements. In the following, we shall assume that the T_1 and T_3 elements are platinum RTDs.

The outside temperature external to the flow sensor may be different than the gas temperature in the flow conduit. For that reason, heat can be conducted in or out of the stems of the velocity sensor and the temperature sensor. In the field, the heat conducted in this manner through each stem may be different from its value at the time of flow calibration if the outside temperatures are different. Additionally, heat can be conducted from the hot velocity sensor to the cooler temperature sensor via their stems. Both effects are further complicated because they depend on the mass flow rate. These phenomena are collectively called “stem conduction.” Stem conduction is a large fraction of the total heat supplied to the velocity sensor and is an unwanted quantity. Left uncorrected, stem conduction constitutes a major source of error in measuring mass flow rate. Flow sensors with long stems have less stem conduction than those with short, stubby stems.

Figure 2(b) shows a thermal dispersion flow sensor that solves the stem conduction problem by employing a total of four platinum RTD temperature sensing elements. The velocity sensor in this “four-temperature” flow sensor has a T_1 element as before, but now has a second T_2 element in its stem separated a short distance from the T_1 element. The temperature sensor has a T_3 element as before, but now has a second T_4 element in its stem separated a distance from the T_3 element. The T_1 element is a wire-wound platinum RTD with a resistance ranging from 10 to 30 Ohms. The T_2 , T_3 , and T_4 sensors are thin-film RTDs with a resistance ranging from 500 to 1000 Ohms. In operation, the T_1 and T_2 elements together act as a heat-flux gauge that measures the fraction of heat conducted down the stem of the velocity sensor. The T_3 and T_4 elements perform the same function for the temperature sensor. The addition of the T_2 and T_4 temperature sensing elements in the “four-temperature” flow sensor facilitates correction for stem conduction, whatever the cause.

The use of the potting material between the T_1 element in Figure 2(a) and the internal surface of the sheath has potential long-term stability problems because the potting material can crack or otherwise

degrade due to differences in the thermal expansion coefficients of the potting material and the sheath material when exposed to gas temperatures that cycle, change frequently, or are elevated. Any change in the potting material causes a change in the “skin resistance” of the velocity sensor and thereby its stability. As discussed in the following, skin resistance, along with stem conduction, are the two major factors that can degrade measurement accuracy if not managed properly.

The construction and assembly of the T_1 element of the four-temperature flow sensor in Figure 2(b) eliminates the skin resistance problem by: (1) avoiding altogether the use of any potting materials between the T_1 element and the internal surface of the sheath and (2) using mating materials that have the same coefficient of thermal expansion. Filler materials are avoided by means of tightly fitting, as in swaging or press fitting, the wire-wound T_1 element into the sheath. Such velocity sensors are known as “dry” sensors, in contrast with velocity sensors fabricated with potting cements or epoxies that are wet when mixed. In contrast with the velocity sensor, any degradation of potting materials in the temperature sensor changes only its time response, a relatively minor effect.

In operation, the gas temperature sensor in the thermal dispersion mass flow meter measures the gas temperature T . The sensor drive in the transmitter electronics delivers an electrical current I_1 to the velocity sensor such that it is self-heated to an average temperature T_1 that is elevated above the gas temperature. Since it is the molecules of the gas, which bear its mass, that flow over the heated velocity sensor and carry away its heat, thermal dispersion flow meters directly measure the mass flow rate q_m of the gas or gas mixture. Heat convected from the velocity sensor in this manner depends on the properties of the gas, and therefore the composition of the gas must be known.

In yet another thermal flow sensor construction for in-line meters, the flow sensor is embedded in wall of the flow body and is not immersed in the flow. This flow sensor consists of a heater element with adjacent upstream and downstream temperature sensing elements. The difference in the two temperatures increases as flow increases, providing the output. This construction is used primarily for low-flow liquid applications.

Transmitter

The transmitter shown in Figure 1 is the electronic system that provides the flow sensor drive and many other functions for the flow meter. It accepts the inputs from the two or four temperature sensing elements as well as the heating current I_1 input and transforms these independent variables into linear outputs of the primary dependent variable, mass flow rate q_m , and, in the case of multivariable versions, the gas

temperature T . The transmitter is housed in an enclosure that conforms with relevant US and international codes, such as hazardous area codes or area classifications. Digital transmitters with digital displays in engineering units facilitate additional functions including flow meter diagnostics, validation, calibration adjustment, and reconfiguration. Later, we describe an advanced system consisting of a microprocessor-based digital transmitter and a four-temperature flow sensor that provides gas selection and automatic correction for changes in gas temperature, gas pressure, and outside temperature.

Many transport properties of the gas that are involved in convective heat transfer, such as thermal conductivity, viscosity, and Prandtl number, depend on temperature. Likewise, the thermal conductivity of some of the materials in the flow sensor depends on temperature. For this reason, thermal dispersion mass flow meters must correct for changes in gas temperature. In traditional flow meters, this is done by means of an analog Wheatstone bridge at the front end of the flow sensor drive. The velocity sensor and the temperature sensor are located at opposite legs of the bridge. This provides compensation for changes in fluid temperature by adjusting the overheat of the velocity sensor. The bridge voltage is a high-level output signal in the order of several volts that provides a high signal-to-noise ratio. The Wheatstone bridge and its temperature-compensation capabilities are thoroughly described in the literature [2, 6-9]. Modern flow meters with a microprocessor-based flow sensor drive digitally correct for changes in temperature without requiring a Wheatstone bridge.

The flow sensor drive in thermal dispersion mass flow meters has two modes of operation: the constant temperature differential mode and the constant current mode. In the constant temperature differential mode of operation, the flow sensor drive maintains at a constant value the difference $\Delta T = T_1 - T$ between the heated velocity sensor T_1 and the gas temperature T . The output signal is the electrical power W supplied to the heated velocity sensor that is required to keep ΔT constant. In the constant current mode of operation, the flow sensor drive maintains at a constant value the current I_1 supplied to the heated velocity sensor. In this case, the output signal is ΔT . Measuring mass flow rate with constant current operation is slower than constant temperature differential operation because the temperature of the entire mass of the velocity sensor must change when velocity changes and also because the masses of the velocity and temperature sensors may be imbalanced. In the following, we assume constant temperature differential operation and that therefore ΔT is a constant, usually in the range of 20 to 100 K.

Liquid Flow Applications

The vast majority of applications are gas flow applications because they benefit from the exceptional low-flow sensitivity and wide rangeability of measurement. Thermal dispersion technology is not well suited

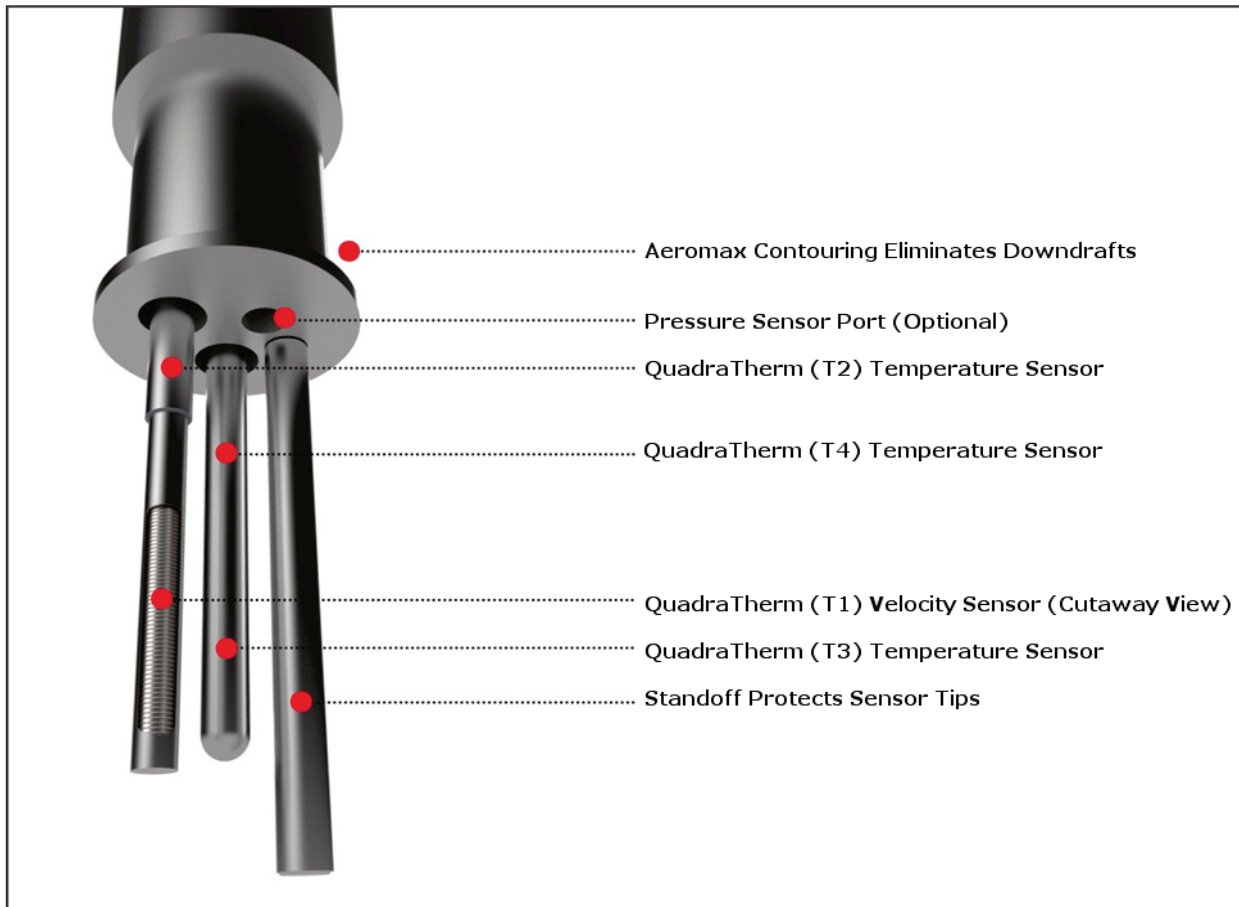


Figure 3 Principle of operation of a four-temperature mass flow sensor with a dry velocity sensor.

for liquid flow applications because at the zero-flow condition, a majority of the heat budget is carried away by the liquid via conduction, instead of the desired convection. This is caused by the high thermal conductivity of liquids relative to gases. The result is reduced measurement sensitivity for liquid flows. Additionally, for liquid flows, the temperature differential $\Delta T = T_1 - T$ must not exceed an upper critical limit, or else at higher flow rates the liquid may flash to the vapor phase and subsequent cavitation may occur, creating unwanted erratic readings. For water flows, this upper critical limit in ΔT is approximately 10 to 20 °C. The constant differential temperature mode of operation is preferred for liquid flows because ΔT is controlled, whereas in the constant current mode ΔT varies and may exceed the upper critical limit. Application of thermal dispersion technology to liquid flows has been limited to cases, such as ultra-low flow applications, where it offers advantages over other technologies.

Principle of Operation

The purpose of this section is to provide a brief description of some of the important principles involved in finding the two output variables—the mass flow rate q_m and the gas temperature T . It is not intended to provide an uninterrupted list of proprietary steps programmed into microprocessor by the manufacturer. Figure 3 shows the principle of operation of the industrial-grade four-temperature thermal dispersion flow sensor with a dry velocity sensor operated in the constant temperature differential mode. The transmitter is the microprocessor-based digital system shown in Figure 4. In the following text, we shall call this flow sensor/transmitter combination the “four-temperature microprocessor-based system.” The fluid is a pure gas or gas mixture of known composition. The following treatment specifically applies to this four-temperature system, but has general applicability to two-temperature systems and liquid flows. Reference 7 specifically applies to hot-wire and hot-film thermal anemometers, but nevertheless is a good back-up source for the principle of operation described here.

The four temperatures are found from the four platinum RTD temperature sensing elements by solving the following equations for temperature

$$R_i = R_{i,o}[1 + A_{1,i}(T_i - T_o) + A_{2,i}(T_i - T_o)^2] \quad (1)$$

Where:

$i = 1, 2, 3, \text{ or } 4$ and refers to one of the four temperature sensing elements

R_i = The electrical resistance of temperature sensing element i at temperature T_i

(Ohms)

$R_{i,o}$ = The electrical resistance of temperature sensing element i at temperature T_o . (Ohms)

T_i = The temperature of sensing element i (K)

T_o = The reference temperature, usually 273.15 (K) [0 (°C)]

$A_{1,i}, A_{2,i}$ = Constants provided by the manufacturer, (K^{-1}) and (K^{-2}) respectively

Equation (1) specifically applies to temperatures T_i above 0 °C. For purposes of the following discussion, we make the following assumption for the T_1 element only

$$R_1 = R_{1,o}[1 + \alpha(T_1 - T_o)] \quad (2)$$

In Equation (2), the term α is the temperature coefficient of resistivity (K^{-1}) and has a value of approximately $0.0039 (K^{-1})$ for platinum RTDs. Equation (2) is quite accurate for gas temperatures in the range of 0 to $100\text{ }^{\circ}C$.

The four-temperature microprocessor-based system measures the primary inputs $R_1, R_2, R_3, R_4,$ and I_1 . It then converts them into secondary inputs $T_1, T_2, T_3,$ and T_4 using Equation (1) and computes the electrical power W supplied to the T_1 heated element using the relationship $W = I_1^2 R_1$ (watts). The transmitter operates in the constant temperature differential mode and therefore maintains the temperature difference $\Delta T = T_1 - T$ at a constant value. The gas pressure P also is an input to the system since the thermal conductivity and other transport properties of gases increase slightly with gas pressure P (bara)—a phenomenon that is often ignored. For pipe lines with nearly constant pressure, this is accomplished by simply inputting that constant pressure. For applications with large excursions in pressure, full multivariable versions with a flow sensor head that also measures the static pressure P provide the needed input. The following text describes the most important relationships needed to convert these inputs into a linear output of mass flow rate q_m and, in the case of multivariable versions, gas temperature T and gas pressure P .

In steady state, the first law of thermodynamics states that the energy (or power) flowing into a defined control volume equals the energy flowing out of the control volume. The control volume to which we shall apply this law is the entire heated section of the velocity sensor. As shown in Figure 3, this cylindrical control volume is enclosed in the dotted lines and is defined by length L_1 and diameter D_1 . It consists of: the cylindrical ceramic mandrel; the R_1 platinum RTD winding around the mandrel that is heated by electrical power W ; and a ceramic or high-temperature glass insulating coating for the winding. The first law for this control volume is

$$W = Q_1 + Q_{tip} + Q_{stem} \quad (3)$$

In Equation (3), Q_{tip} and Q_{stem} are the heat rates (watts) conducted from the control volume to the tip and stem of the velocity sensor, respectively. Collectively, they constitute the heat rate lost via the previously mentioned “stem conduction.” Q_1 is the heat rate (watts) transferred from the heated control volume to the flowing gas by natural and forced convection and by radiation. Q_1 is expressed as

$$Q_1 = h_c(\pi D L_1) \Delta T \quad (4)$$

In Equation (4), D is the outside diameter (m) of length L_1 (m) of the velocity sensor. h_e is the effective film coefficient for convection (watts/m²/K), defined as

$$h_e = \frac{h}{1 + h\pi DL_1 R_{skin}} \quad (5)$$

Where:

h = The film coefficient for convection averaged over the surface of the heated section of the velocity sensor (watts/m²/K)

R_{skin} = The skin resistance described below (K/watt)

In Equation (5), we have ignored radiative heat transfer because it is negligible, except when the gas temperature is very high. The average temperature T_e of the external surface of the velocity sensor over length L_1 , shown in Figure 3, is less than the average temperature T_1 of the control volume. This is due to the temperature drop that is required to pass the heat rate Q_1 through the intervening layers of material between the control volume and its external surface. These intervening layers are called the “skin.” R_{skin} is the average thermal resistance of the skin over length L_1 , i.e., the “skin resistance,” and is defined by

$$Q_1 = \frac{(T_1 - T_e)}{R_{skin}} \quad (6)$$

As evidenced by Equation (5), at higher flow rates and thus higher values of h , the skin resistance R_{skin} causes a drop in the output signal and consequently a reduction in sensitivity. This is why skin resistance is an unwanted quantity that should be minimized in flow sensor design; should not change over time; and should be measured by the flow meter.

R_{skin} is the sum of the thermal resistances of the annular layers in the skin of the velocity sensor and is calculated as follows

$$R_{skin} = \left(\frac{1}{2\pi L_1}\right) \sum_{j=1}^n \left[\frac{\ln\left(\frac{D_{j+1}}{D_j}\right)}{k_j} \right] \quad (7)$$

In the above, n is the total number of layers in the skin; $j = 1, \dots, n$; D_j and D_{j+1} are the inside and outside diameters of layer j , respectively ($D_1 < \dots < D_{n+1} = D$); and k_j is the thermal conductivity of layer j . The two-temperature flow sensor shown in Figure 2(a) has three layers in the skin of the velocity sensor—the thin insulation layer over the platinum RTD; the potting material; and the sheath. The four-temperature flow sensor in Figure 2(b) also has three layers in the skin of the velocity sensor—the thin insulation layer over

the platinum RTD winding; a very thin air gap with an average thickness in the order of 0.005 mm [0.0002 inches]; and the sheath. The thin air gap in the velocity sensor of the four-temperature version exists because, although the mating parts are in contact via their press fit, slight imperfections in their circularity can cause thin air gaps over a fraction of the mating surface. R_{skin} ranges from 3 to 10 watts/K for two-temperature flow sensors and from 2 to 5 watts/K for four-temperature flow sensors.

The four-temperature microprocessor-based system solves for h and T . Given h and T , the next step in finding the mass flow rate q_m is to find the Reynolds number Re using an empirical correlation for convective heat transfer. This correlation has the following two forms, depending upon whether it is solved for the Nusselt number Nu or the Reynolds number Re

$$Nu = F(Re, Pr) \quad \text{and} \quad Re = G(Nu, Pr) \quad (8)$$

Where:

$Nu = \frac{hD}{k}$ = Nusselt number, the non-dimensional heat-transfer parameter

$Re = \frac{\rho VD}{\mu}$ = Reynolds number, the non-dimensional ratio of dynamic forces to viscous forces, based on the outside diameter D of the velocity sensor

$Pr = \frac{\mu c_p}{k}$ = Prandtl number, the non-dimensional ratio of the diffusivity of momentum to the diffusivity of heat

k = The thermal conductivity of the gas (watts/m/K)

ρ = The mass density of the gas (kg/m^3)

μ = The absolute viscosity of the gas (kg/s/m)

c_p = The coefficient of specific heat of the gas at constant pressure (J/kg/K)

A typical example of the two forms of the correlation is

$$Nu = b_1 + b_2 Pr^{b_3} Re^{b_4} \quad \text{and} \quad Re = \left[\frac{Nu - b_1}{b_2 Pr^{b_3}} \right]^{1/b_4} \quad (9)$$

Where:

b_i = Dimensionless constants, $i = 1, 2, 3,$ or 4

In Equations (8) and (9), all properties and dimensions refer to the velocity sensor. In the above, we have assumed that the flow: is non-zero; is in the continuum flow regime (i.e., is not in a high vacuum); and is incompressible (i.e., the Mach number is less than approximately 0.3).

The law of conservation of mass (the continuity equation) requires that

$$\rho V = \rho_s V_s \quad (10)$$

In Equation (10), V is the actual velocity (m/s) measured at the midpoint of the heated section of the velocity sensor, often called the “point velocity”. The subscript ()_s refers to standard, or base, conditions of standard temperature T_s and absolute pressure P_s . Many applications use standard conditions of: $T_s = 70 \text{ }^\circ\text{F} = 21.11 \text{ }^\circ\text{C} = 294.26 \text{ K}$ and $P_s = 1 \text{ atmosphere} = 101325 \text{ Pa} = 1.01325 \text{ bara}$. Another class of applications uses standard conditions, often called “normal” conditions, of: $T_s = 0 \text{ }^\circ\text{C} = 273.15 \text{ K}$ and

$P_s = 1 \text{ atmosphere} = 1.01325 \text{ bara}$.

The constant standard mass density ρ_s (kg/standard m^3) for gases obeying a modified perfect gas law equation of state is calculated as follows

$$\rho_s = \frac{P_s M}{z_s R T_s} \quad (11)$$

Where:

M = The molecular weight of the pure gas or gas mixture (kg/kg-mole)

R = The universal gas constant ($\text{m}^3 \cdot \text{bara}/\text{kg-mole}/\text{K}$)

z_s = The dimensionless compressibility of the gas at standard conditions

In Equation (11), P_s and T_s are the standard absolute pressure (bara) and the standard absolute temperature (K) of the gas, respectively. In full multivariable versions that provide an in situ measurement the gas pressure P , the actual mass density ρ of the gas can be outputted using Equation (11), modified by removing the subscripts ()_s.

Based on Equation (10), the Reynolds number Re defined in Equation (8) also can be expressed as

$$\text{Re} = \frac{\rho_s V_s D}{\mu} \quad (12)$$

From Equations (8) and (12), we arrive at

$$V_s = \left(\frac{\mu}{\rho_s D}\right) G(\text{Nu}, \text{Pr}) \quad (13)$$

In the above, V_s is called the point “mass velocity” (standard m/s) because when it is multiplied by the constant mass density ρ_s , it yields the mass flow rate per unit area at a point (or small area) in the cross-sectional area of the flow conduit. This is the mathematical reason why thermal dispersion mass flow meters directly measure mass flow rate.

In most insertion flow meter applications, the desired final output variable is the mass velocity V_s (standard m/s). In this case, V_s is calculated using Equation (13). If the desired output is the actual velocity V (m/s), then V is found from $V = (\rho_s/\rho)V_s$. If the desired final output is the total mass flow rate q_m (kg/s) flowing through a pipe or other flow conduit, then the following relationship is used

$$q_m = (F_c A_{\text{pipe}}) \rho_s V_s \quad (14)$$

In Equation (14), A_{pipe} is the cross-sectional area (m^2) of the pipe or flow conduit, and the term F_c is defined as $F_c = V_{s,\text{ave}}/V_s$, where $V_{s,\text{ave}}$ is the average mass velocity (standard m/s) over the cross-sectional area A_{pipe} . Most insertion meters are inserted such that the midpoint of the heated section of the velocity sensor is at the center line of the pipe. In this case and with a fully developed velocity profile in the pipe, typical values of F_c are: $F_c = 0.5$ for $\text{Re}_{\text{pipe}} \leq 2,000$, and $F_c = 0.83 \pm 0.03$ (depending on the roughness of the internal surface of the pipe) for $\text{Re}_{\text{pipe}} \geq 40,000$, where Re_{pipe} is the Reynolds number based on the internal diameter of the pipe [10]. For in-line meters, Equation (14) is not used explicitly. Instead, the factor $(F_c A_{\text{pipe}})$ becomes a meter factor determined via flow calibration. Tables 1 and 2 provide a list of the formulas used by the four-temperature microprocessor-based system to calculate the output variables of insertion meters and in-line meters, respectively.

Advanced Four-Temperature Microprocessor-Based System

Figure 4 shows a simplified block diagram of the microprocessor-based thermal dispersion mass flow meter with the four-temperature flow sensor shown in Figure 2(b). It has a dry velocity sensor and is operated in the constant temperature differential mode. As before, we call this configuration the four-temperature microprocessor-based system. The voltage sensing wires in Figure 4 make the measurement of the RTD resistances independent of the length of the flow sensor cable, facilitating remote location of

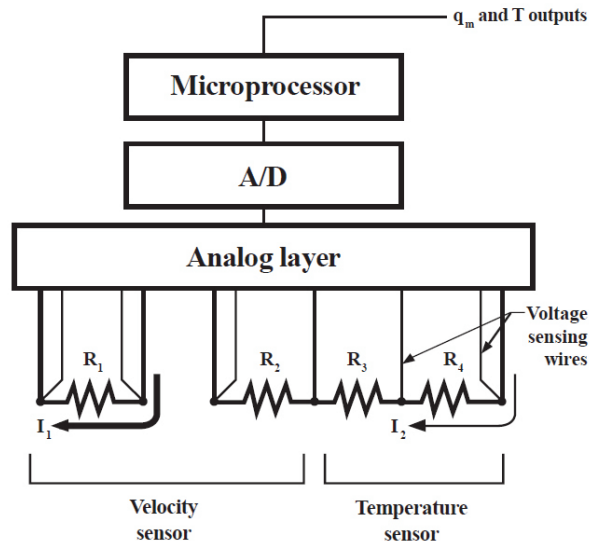


Figure 4 The four-temperature microprocessor-based system. The flow meter drives the velocity sensor so that the temperature difference $\Delta T = T_1 - T_2$ is maintained constant. The system automatically corrects for changes in gas selection, gas temperature, and gas pressure.

the transmitter. The heating current I_1 depends on the electrical resistance R_1 and the electrical power input W required to maintain ΔT constant. W ranges from about 0.2 to 5 watts depending on the overheat ΔT , the mass flow rate, and the size of the velocity sensor. The temperature sensing current I_2 is held constant and is less than 1 mA to avoid self-heating the T_2 sensor. The analog layer shown in Figure 4 includes precision resistors for measuring the currents I_1 and I_2 but has no bridge circuit.

The four-temperature microprocessor-based system shown in Figure 4 digitally linearizes the q_m output and, optionally, the T and P outputs and provides analog outputs for these variables. The system has algorithms based on the above principle of operation that manage changes in gas selection, gas temperature, and gas pressure. It also provides a selection of digital communication protocols, including Hart, Foundation Fieldbus, and Profibus (all trademarked). The system enables a number of traditional digital functions, such as: a multi-variable digital readout and user interface; digital RS 232 and RS 485 communications; flow meter diagnostics, validation, calibration adjustment, and reconfiguration; flow totalization; and alarms.

Figures 5(a), 5(b), and 5(c) show how the four-temperature microprocessor-based system manages changes in gas selection, gas temperature, and gas pressure for air, methane, and argon. These figures are plotted in the conventional manner with the mass velocity V_s shown as the independent variable and the electrical power W shown as the dependent variable, whereas in the system they have reversed roles. The three figures reflect the strong direct dependence the electrical power W has on the thermal conductivity

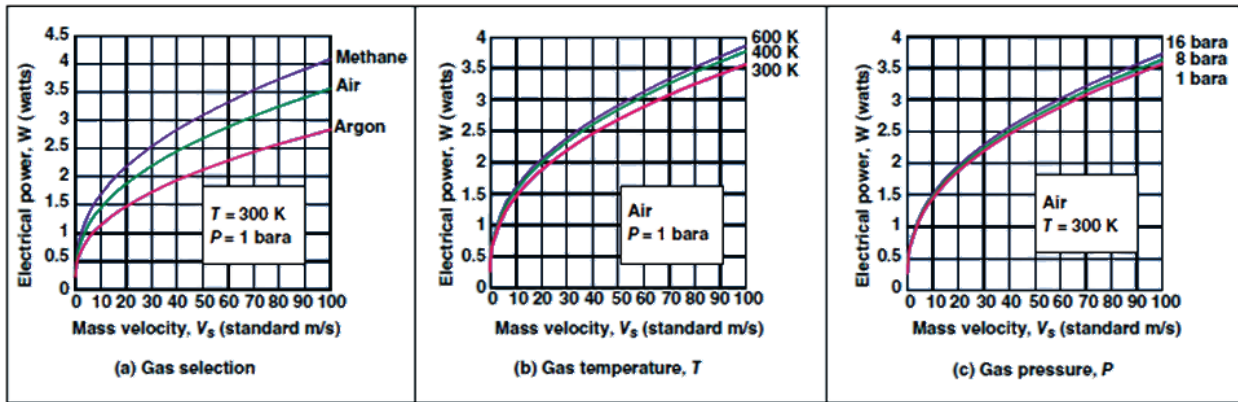


Figure 5 Management of changes in gas selection, gas temperature, and gas pressure with the four-temperature microprocessor-based system. $\Delta T = 50$ K. In all figures the “standard” conditions for V_s (standard m/s) are 70°F and 1 atmosphere .

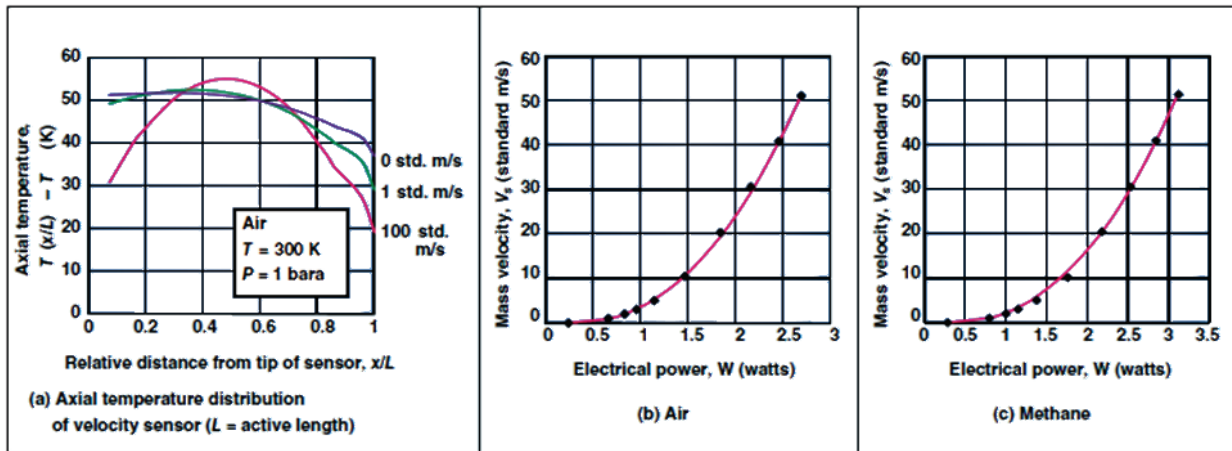


Figure 6 Comparison between flow calibration data and the output of the four-temperature microprocessor-based system. $\Delta T = 50$ K, and T and P are at room (ambient) conditions. “Standard” conditions for V_s (standard m/s) are 70°F and 1 atmosphere.

of the gases. Thus, Figure 5 (a) results from the fact that $k_{methane} > k_{air} > k_{argon}$, and Figures 5(b) and 5(c) result from the fact that thermal conductivity increases as gas temperature and pressure increase, respectively. The fact that thermal conductivity, and therefore W , increases with gas pressure as shown in Figure 5(c) is a phenomenon that has heretofore been ignored, but for higher accuracy applications should be included.

Figures 5(a), 5(b), and 5(c) also reveal the non-linear, logarithmic nature of the output. A log vs log plot of these figures will reveal a nearly straight line over approximately 1 to 150 standard m/s. This logarithmic property is responsible for the exceptional rangeability and low-velocity sensitivity of thermal

Table 3 Typical specifications for thermal dispersion mass flow meters

Specification	Two-temperature system	Four-temperature system
Gases	Most clean gases, including Natural Gas, Air, Methane, Ar, CO ₂ , He, N ₂ , O ₂ , C ₃ H ₈ , and mixtures of these components	Most clean gases, including Natural Gas, Air, Methane, Ar, CO ₂ , He, N ₂ , O ₂ , C ₃ H ₈ , and mixtures of these components
In-line flow body sizes ^a	0.25, 0.5, 1.0, 1.5, 2.0, 4.0 inches; DN6 to DN100	0.25, 0.5, 1.0, 1.5, 2.0, 4.0 inches; DN6 to DN100
In-line meter mass flow rate range for air Insertion meter mass velocity range for air	0.0001 to 1.5 kg/s; 0.1 to 2600 scfm ^b 1.4 to 140 normal m/s; 300 to 30,000 standard ft/min ^c	0 to 1.5 kg/s; 0 to 2600 scfm ^b 0 to 140 normal m/s; 0 to 30,000 standard ft/min ^c
Temperature range ^d	-40 to 200 °C; -40 to 392 °F	-40 to 200 °C; -40 to 392 °F
Pressure range	0.01 to 16 bara	0.01 to 16 bara
Accuracy ^e	±1 % of reading plus 0.5 % of full scale	±1 % of reading from 10 to 100 % FS; ± 1 % of reading plus 0.5 % FS from 0 to 10 % FS
Rangeability	100 : 1	100 : 1
Repeatability	±0.2 % of full scale	±0.15 % of full scale
Time response ^f	3 sec (constant power operation); 1.2 sec (constant ΔT operation)	2 sec
Stability	1 year; typical drift 1 to 2 % per year	10 years; typical drift 0.1 % per year

Notes to Table 3: (a) Some manufacturers offer sizes up to 12.0 inches (DN300); (b) Based on the point mass velocity range for insertion flow meters cited below; (c) “Normal” conditions are 0 °C and 1 atmosphere, and “standard” conditions are 70 °F and 1 atmosphere; (d) High temperature models are available up to approximately 450 °C = 842 °F; (e) FS = full scale; and (f) Time Response is the time required to reach 63 % of the final value (i.e., the 1 sigma value).

dispersion mass flow meters. A rangeability as high as 100:1 is common. Even higher rangeabilities are achieved with multi-range flow calibration. Detectable minimum point mass velocities as low as approximately 0.1 standard m/s (20 standard ft/min) are reported by some manufacturers. In the early days of analog electronics, it was difficult to linearize the output of thermal dispersion mass flow meters. But now, with microprocessor-based electronics, it is not a problem, and the non-linear, logarithmic nature of the output bears only advantages.

Figures 5(d) and 6 show further results of the four-temperature microprocessor –based system. Figure 5(d) reveals how the temperature distribution $T_1(x)$ of the heated section of the velocity sensor undergoes

major changes as the mass velocity V_s increases from 0 to 100 standard m/s. Figures 6(a) and 6(b) show, for air and methane, the excellent comparison between results calculated via the four-temperature

microprocessor-based system and actual flow calibration data. Comparisons for other gases are likewise as good. Algorithms exist that make the output of the system match flow calibration data even better.

Specifications

Table 3 shows specifications for currently available thermal dispersion mass flow meters. Specifications for the column labeled “Two-temperature system” refer to the flow sensor shown in Figure 2(a) and may vary from manufacturer to manufacturer. Specifications for the column labeled “Four-temperature system” refer to the microprocessor-based system with the four-temperature flow sensor having the dry velocity sensor shown in Figure 2(b). Accuracy specifications in Table 3 may apply to gas temperatures and gas pressures that lie within bands around their respective values at flow calibration. Table 3 is also useful in selecting and sizing the proper thermal dispersion mass flow meter for the application.

Conclusion

Flow meters based on thermal-dispersion technology directly measure the mass flow rate of gases in rugged industrial-grade applications. The advanced thermal dispersion mass flow meter described in this article has a flow sensor with four platinum RTD temperature sensing elements, instead of the traditional two. This unique four-temperature configuration facilitates, for the first time, the essential measurement of the fraction of heat conducted through the stems of the velocity and temperature sensors. Unlike traditional flow sensors, the advanced flow sensor has a dry velocity sensor that has no potting material between its heated element and its sheath. This solves the common skin resistance problem by eliminating the cracking and degradation associated with potting materials that ultimately compromise stability and accuracy. Finally, the advanced flow sensor of insertion flow meters has an innovative design that makes accuracy independent of insertion depth.

The advanced thermal dispersion mass flow meter couples the new flow sensor with microprocessor-based electronics programmed with proprietary algorithms that manage any changes in gas selection, gas temperature, gas pressure, and outside temperature. Multivariable versions provide analog and digital outputs of mass flow rate, gas temperature, and gas pressure. A selection of sophisticated digital communication protocols commonly used by industry is available.

Acknowledgement

The author wishes to thank John Smitherman and Brian Estep of the Sierra Instruments engineering team for their major contributions to this work.

References

1. King, L. V. 1914. On the convection of heat from small cylinders in a stream of fluid: Determination of the convection constants of small platinum wires with application to hot-wire anemometry. *Phil. Trans. Roy. Soc.* A214: 373-432.
2. Olin, J. G. 1999. Thermal anemometry. In *The Measurements, Instrumentation, and Sensors Handbook*, ed. Webster, J. G., 29-18 to 29-37. Boca Raton: CRC Press.
3. ASME MFC-21.2-2010. Measurement of fluid flow by means of thermal dispersion mass flowmeters.
4. ASME MFC-21.1M. Measurement of fluid flow by means of capillary tube thermal mass flowmeters and controllers.
5. ASME MFC-15M. Insertion metering.
6. Olin, J. G. 1993. A thermal mass flow monitor for continuous emissions monitoring systems (CEMS). *Proc. ISA/93 International Conference, Exhibition and Training Program.* 93-404: 1635-1653.
7. Bruun, H. H. 1995. *Hot-Wire Anemometry: Principles and Signal Analysis*. Oxford: Oxford Univ. Press.
8. Olin, J. G. 1999. Industrial thermal mass flowmeters—Part 1: Principles of operation. *Measurements and Control.* 193 (Feb.): 83-90.
9. Olin, J. G. 1999. Industrial thermal mass flowmeters—Part 2: Applications. *Measurements and Control.* 194 (Apr.): 1-6.
10. Miller, R. W. 1996. *Flow Measurement Engineering Handbook. 3rd Ed.* McGraw-Hill.



About the Author



John G. Olin, Ph.D., is the founder and chairman of Sierra Instruments, Inc., located in Monterey, Calif. Dr. Olin received his bachelor's degree from Illinois Institute of Technology and his master's and Ph.D. from Stanford University, all in Mechanical Engineering. At Stanford, Dr. Olin specialized in fluid mechanics and heat transfer and used thermal flow meters in research pursuant to his doctoral dissertation. He founded Sierra Instruments in 1973 with the purpose of offering thermal mass flowmeters to solve industry's need for accurate, reliable flowmeters based on the thermal principle. Dr. Olin has a dozen patents and over 60 papers in the field.